FTD-ID(RS)T-0572-91

# FOREIGN TECHNOLOGY DIVISION

POGO STABILITY, RELIABILITY AND PARAMETERS ANALYSIS

by

Qizheng Wang, Wanyong Gau, et. al.



Approved for public release;
Distribution unlimited.

# HUMAN TRANSLATION

FTD-ID(RS)T-0572-91 19 November 1991

POGO STABILITY, RELIABILITY AND PARAMETERS ANALYSIS

By: Qizheng, Wang, Wanyong Gau, et. al.

English pages: 49

Source: Yuhang, Xuebao, NR 2, 1986, pp. 29-47

Country of origin: China
Translated by: SCITRAN
F33657-84-D-0165
Requester: FTD/TTTAV/A. G. Crowder




PREPARED BY:

TRANSLATION DIVISION
FOREIGN TECHNOLOGY DIVISION
WPAFB. OHIO.

## GRAPHICS DISCLAIMER

All figures, graphics, tables, equations, etc. merged into this translation were extracted from the best quality copy available.

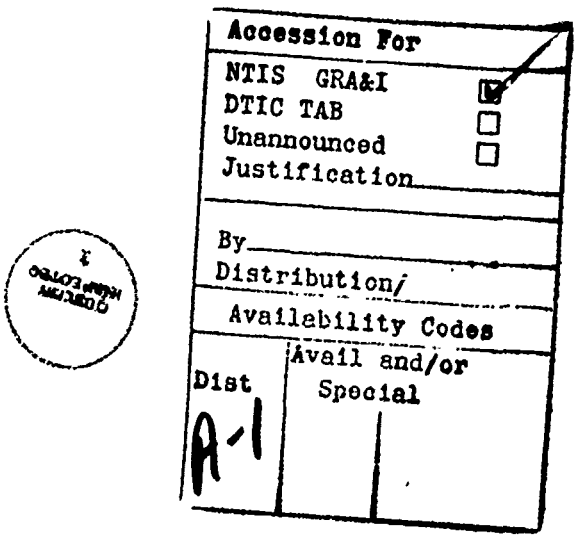

# POGO STABILITY, RELIABILITY AND PARAMETERS ANALYSIS

Wang, Qizheng; Gau, Wanyong; Gu, Yongchun; Zhang, Jitony;
and Li, Xianshan

Abstract POGO instability is one of the most important dynamical problems of space vehicles. The mechanism of the POGO instability is briefly clarified by a simple free-free system which consists of two masses, a spring, and a damper, followed by POGO stability matrix algorithm, POGO stability single-transfer method, and POGO stability estimation method. The adaptability of these POGO stability analysis is illustrated through an example. After important parameters related to POGO instability are discussed, the reliability analysis of POGO stability and its criteria are also introduced.

(This paper was received on September 6, 1984.)

## I. Mechanism of POGO Instability

The phenomenon of POGO not only has adverse effect on the passenger-carrying space vehicles, it is also an important element in structural design. The high pressure vibration in the propellent line caused by POGO can result in the degradation of the performance of the propulsion system, and sometimes even pre-mature engine shut-down [1,2].

In the 70's, the suppression of POGO instability was viewed as one of the most important criteria in the design of gas-liquid structural system and manned space vehicle. In the 80's, it was

still a part of the research of space-traveling related structural dynamics [3].

Similar to flutter and galloping in the gas elasticity, POGO is an important problem in the fluid-solid coupled dynamics. Flutter and galloping are the dynamic problems caused by the flowing of fluid exterior of a solid, while POGO is the dynamic problem caused by the flowing of fluid interior of a solid. Since the structural vibration is a three-dimensional problem, and the pipeline system in real space consists of pipelines in all three dimensions which is further controlled by the propulsion of the engine and other controlling forces, POGO is the dynamic problem of a large-loop coupling system.

POGO is the study of structural instability of the rocket body structural system and the longitudinal coupling of the propulsion system. Under the condition of POGO, longitudinal self-stimulating non-convergent vibration of the space vehicle is caused which is similar to the ever-jumping "pogo stick" and hence was given the name.

The stability of POGO was already discussed in literatures [4] to [7]. In the past, the mechanism of POGO was mostly discussed in words or through complicated calculation. Similar to the mechanism of flutter [8], POGO can be explained by the system of two free-free masses($M_1$, $M_2$) - damper($C_2$) - spring($K_2$). From figure 1.1b, we have

$$M_1\ddot{X}_1+C_2(\dot{X}_1-\dot{X}_2)+K_2(X_1-X_2)=F_1(t) \tag{1.1}$$

$$M_2\ddot{X}_2+C_2(\dot{X}_2-\dot{X}_1)+K_2(X_2-X_1)=0 \tag{1.2}$$

let $\delta=X_1-X_2$, $\omega_2^2=K_2(M_1+M_2)/(M_1M_2)$

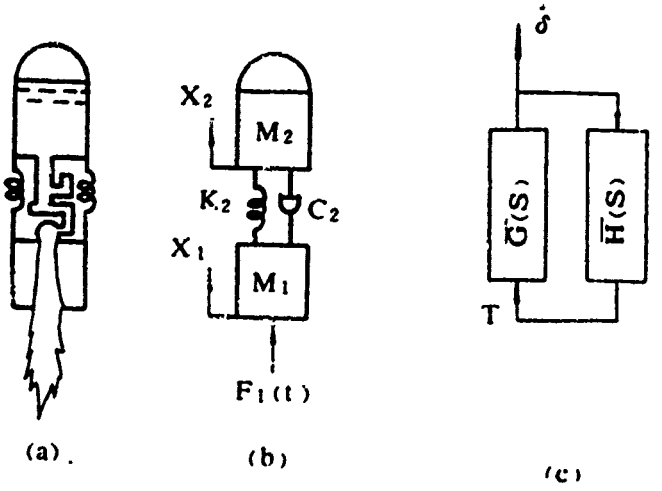


Fig 1.1

$$2\zeta_n\omega_n = C_s(M_1 + M_2)/(M_1M_2) \tag{1.3}$$

Assuming that the pulse thrust $\overset{\backsim}{F}_1(t)$ is proportional to the relative deformation velocity $\dot{\delta}$. then

$$T = F_1(t)/M_1 = 2\zeta_e\omega_n\dot{\delta} \tag{1.4}$$

where $\zeta_e$ is related to many factors of the propulsion system. Using the above equation. we have

$$\ddot{\delta} + 2\omega_n(\zeta_n - \zeta_e)\dot{\delta} + \omega_n^2\delta = 0 \tag{1.5}$$

If the initial perturbation is $\delta_0$, then the solution can be $\delta = \delta_0 e^{st}$, and we have

$$S^2 + 2\omega_n(\zeta_n - \zeta_e)S + \omega_n^2 = 0 \tag{1.6}$$

the roots are

$$S_{1,2} = -(\zeta_n - \zeta_e)\omega_n \pm j\omega_n\sqrt{1-(\zeta_n-\zeta_e)^2} \tag{1.7}$$

and the solution is therefore.

$$\delta = \delta_0 EXP[-(\zeta_n - \zeta_e)\omega_n t]\cos(\omega_d t + \theta_0) \tag{1.8}$$

where $\omega_d = \omega_n\sqrt{1-(\zeta_n-\zeta_e)^2}$;

$\theta_0$ is a constant.

If equation (1.8) is plugged into equations (1.1) to (1.3). then the reverse motion of $X_1$ and $X_2$ can be realized. If the actual structural modular damping ratio $\zeta_n$ is a positive damping. then when

$\zeta=\zeta_a-\zeta_e<0$ then the unstable divergent vibration due to the negative damping of the system will occur. In this case. the system will absorb energy and the source of energy is the work of pump and engine. This is similar to the flutter of wings of aircraft. even though the engine provide the flight speed to the aircraft. not all the flight speed will cause unstable flutter of the wings. For POGO systems. only under certain coupling conditions which render large $\zeta_e$ can unstable pogo occur and the extent of instability if determined by the magnitude of $\zeta$. The magnitude of $\zeta_e$ is further determined by structure, pump, and the closeness of the gain of the engine and the characteristic frequency of the propellant line. The latter is an important design criterion of POGO (see section V.3). If coupling is removed by some measures. $\zeta_e$ can be reduced and system POGO can be avoided.

As mentioned above. POGO of space vehicles is a problem of the large-loop coupling dynamics. Since the structure of space vehicles consisted of many modules. many propellants. many pipelines. and the simultaneous working of pump and engine. some local vibration can also cause POGO. therefore. the dynamic equations for many parts can be generated (see section II). Then the dynamic polynomials of the entire POGO system can be tabulated and then the calculation of the POGO stability of the entire system can be carried out (see section III). However, since the physical significance is hard to detect in the initial stage of calculation. the POGO single-transfer and estimation methods should be used (see section IV) to estimate the POGO stability of the vehicle in a more efficient way. Nevertheless. the relative error should be noted in the estimation procedure.

There are many factors affecting POGO. If the major factors are identified, the requirements for the system design, test, planning, and quality control can be outlined (see section V). Furthermore, there are some uncertain parameters in the POGO stability analysis and the reliability analysis (section VI) and the POGO reliability requirement which suppresses POGO (section VII) should be carried out.

## II. The Related Dynamic Equations of a POGO System

The typical block diagram of the simplified coupling of propulsion-structure system is shown in figure 4.1. Four major sub-systems are shown: structural system of the vehicle, propellant pipeline system, pump system, and the thrust chamber system. The description of these systems is followed.

(I) Dynamic equations of the vehicle structural system

The dynamic equations for the ith degree modular state are

$$X_i(e) = G_{ie}(S)T_i(e) \tag{2.1.1}$$

$$G_{ie}(S) = SG_i(e)/(S^2 + 2\zeta_i\omega_i S + \omega_i^2) \tag{2.1.2}$$

$$G_i(e) = \phi_i^2(e)/M_i \tag{2.1.3}$$

$$T_i(e) = \frac{1}{\phi_i(e)} \sum F(j)\phi_i(j) \tag{2.1.4}$$

where $\zeta_i$, $M_i$, $\omega_i$, $\phi_i(j)$, $\phi_i(e)$, and $G_i(e)$ are the modular damping ratio, macroscopic mass, circular frequency of the ith modular state, the modular displacement of the jth point, general modular displacement of the engine, and structural gain. F(j) is the external force applied on point j of the rocket body. The physical displacement of the jth point on the structure is

$$X(j)=\sum_{i=1} X_i(j)=\sum_{i=1} \phi_i(j)\, q_i e^{i\omega t} \qquad (2.1.5)$$

where $q_i$ is the macroscopic coordinate. The form of the typical external force F(j) is explained below.

1. The pulse thrust F(1) created by the pulse pressure Pc of the combustion chamber on the engine is

$$F(1)=A_{th}C_f P_c=S_e P_c \qquad (2.1.6)$$

where $S_e=A_{th}C_f$. and $A_{th}$ and $C_f$ are the cross section of the neck of the combustion chamber and thrust coefficient.

2. The forces F(2) and F(3) applied on the structure as a result of the pulse pressure due to elbow or pipelines before/after a pump and momentum change are (see figure 2.3)

$$F(2)=-A_U P_U-\rho\bar{Q}_U(2Q_U/A_U+\dot{X}_b) \qquad (2.1.7)$$

$$F(3)=-A_D P_D-\rho\bar{Q}_D(2Q_D/A_D-\dot{Y}_b) \qquad (2.1.8)$$

where $A_U$, $P_U$, $\bar{Q}_U$, $Q_U$ are the inlet cross section. pulse pressure. steady state and pulsed volume flow of the upstream flow: and $A_D$. $P_D$. $\bar{Q}_D$, $Q_D$ are the corresponding quantities of the downstream flow. $\dot{X}_b$ and $\dot{Y}_b$ are the transverse and longitudinal velocity at the elbow or pump.

3. Due to change in cross sectional area, the change in pressure and momentum result in an applied force on the structure F(4) (see figure 2.4) is

$$F(4)=-A_U P_U+A_D P_D-2\rho\bar{Q}\left(\frac{Q_U}{A_U}-\frac{Q_D}{A_D}\right) \qquad (2.1.9)$$

4. The applied force F(5) as a result of the viscosity of the fluid in a straight line (see figure 2.1) is

$$F(5)=-\frac{AR}{Z}(P_U-P_D+SLA\dot{X}_l) \tag{2.1.10}$$

where A. R. Z. L. $\dot{X}_l$ are the corresponding cross sectional area, resistance, impedance, inertia, and velocity.

5. The applied force created by the pulsed flow $Q_R$ of the propellent on the bottom of the fuel tank on the center-of-mass of the fuel tank with respect to the structure is

$$F(6)=\rho h_t \dot{Q}_R \tag{2.1.11}$$

where $h_t$ is the height of the liquid in the fuel tank.

6. The applied force F(7) created by the pulsed pressure Pt at the opening (tb) at the bottom of the fuel tank on the bottom structure is [6]

$$F(7)=A_1 P_t \tag{2.1.12}$$

where

$$P_t=\sum_{K=1}\rho h_t \phi_K(f)\ddot{q}_K-L_t\dot{Q}_R \tag{2.1.13}$$

$$Q_R=Q_t+A_1\dot{X}(tb)=Q_t+A_1\sum_{K=1}\phi_K(tb)\dot{q}_K \tag{2.1.14}$$

where $\phi_K(f)$, $\phi_K(tb)$, and $L_t$ are the modular displacement of the center-of-mass of the liquid reservoir, the modular displacement of the bottom of the tank, and inertia of the liquid in the tank. $A_1$ is the area of the opening, and $Q_R$ and $Q_t$ are the relative and true flow rate.

7. The force F(8) acting on the structure of the rocket body as a result of the local. longitudinal motion of the pump is

$$F(8)=M_p[\ddot{X}(tp)-\ddot{X}_p] \qquad (2.1.15)$$

where $\ddot{X}$(tp) is the acceleration of the pump component of the rocket structure. $\ddot{X}_p$ is the acceleration due to local longitudinal motion of the pump. and $M_p$ is the mass of the pump component.

(II) Dynamic equations of the pipeline sections

1. straight pipeline sections (see figure 2.1)

Assuming that the steady state velocity in the pipeline is much less than the speed-of-sound. then the effect of Mach number can be ignored and the following relationship holds

$$\begin{Bmatrix} P_D \\ Q_D \end{Bmatrix}=\begin{bmatrix} ch\theta & -\frac{1}{\theta}Zsh\theta \\ -\frac{1}{Z}\theta sh\theta & ch\theta \end{bmatrix}\begin{Bmatrix} P_U \\ Q_U \end{Bmatrix}-\begin{Bmatrix} \frac{1}{\theta}ARsh\theta \\ \frac{AR}{Z}(1-ch\theta) \end{Bmatrix}\ddot{X}_t \qquad (2.2.1)$$

where $\theta'=S'\tau'Z/(SL)$; $\tau=l/a_e$ : l is the length of the pipeline.

$L=\rho l/A$; $Z=R+SL$ : $a_e$ is the equivalent speed-of-sound (see discussions in section V(6)).

If the effect of viscosity can be ignored than R is approximately zero and the above equation has the following form

$$\begin{Bmatrix} P_D \\ Q_D \end{Bmatrix}=\begin{bmatrix} ch(\tau s) & -\frac{Lsh(\tau s)}{\tau} \\ -\frac{\tau sh(\tau s)}{L} & ch(\tau s) \end{bmatrix}\begin{Bmatrix} P_U \\ Q_U \end{Bmatrix} \qquad (2.2.2)$$

If the effect of compressibility can be ignored. then $a_e$ approaches infinity and the above equation is further simplified as

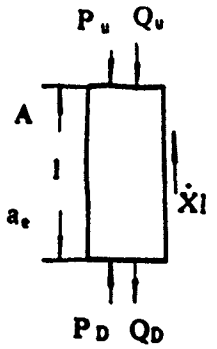


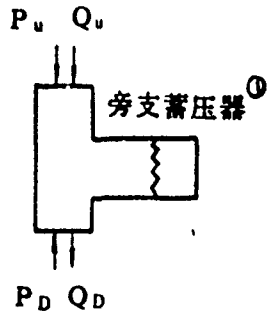


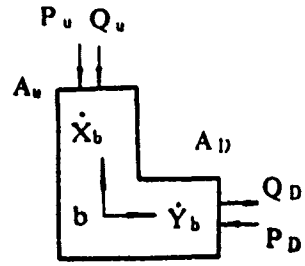


key: 1 - bypass pressure retainer

Fig 2.1

Fig. 2.2

Fig. 2.3

$$\begin{Bmatrix} P_D \\ Q_D \end{Bmatrix} = \begin{bmatrix} 1 & -SL \\ 0 & 1 \end{bmatrix} \begin{Bmatrix} P_U \\ P_U \end{Bmatrix} \tag{2.2.3}$$

2. If the pipeline system is complicated and the gas content of the liquid and the gas bubble generated during flow of the liquid can not be estimated easily, then the calculation of equivalent speed-of-sound is made very difficult and the modular parameters of the pipeline system can be estimated by the trial method. For example, when the two ends of the pipeline connecting the bottom of the liquid reservoir and the pump is closed/opened, then we have

$$(S^2 + 2\zeta_l \omega_l S + \omega_l^2) q_l = A_l P_U / M_l \tag{2.2.4}$$

When the two ends are closed/closed, then

$$(S^2 + 2\zeta_l \omega_l S + \omega_l^2) q_l = -A_l (P_U + P_D) / M_l \tag{2.2.5}$$

where $\zeta_l$, $\omega_l$, $M_l$, $q_l$, . are the modular damping ratio, circular frequency, macroscopic mass, and macroscopic coordinate of the pipeline.

3. The equation for the pressure retainer (or connecting between branches) is (see figure 2.2)

$$\begin{Bmatrix} P_D \\ Q_D \end{Bmatrix} = \begin{bmatrix} 1 & 0 \\ -Y_a & 1 \end{bmatrix} \begin{Bmatrix} P_U \\ Q_U \end{Bmatrix} \tag{2.2.6}$$

where

$$Ya = SC_a / (LaCaS^2 + R_a C_a S + 1); \tag{2.2.7}$$

$$L_a = \rho l_l / A_a; \quad l_e = l_a + 8r_a/(3\pi); \quad A_a = \pi n_a r_a^2 \tag{2.2.8}$$

$$C_e = V/(\gamma P) = \begin{cases} V_a P_a / (\gamma P^2) & \text{(isothermal process)} \end{cases}$$

(2.2.9)

$$C_p = V_0 \gamma / P_0 / P / (\gamma P) \quad \text{(adiabatic process)}$$

$$R_a = \sqrt{\Delta P / K};\ K = 2\rho g^2 (C_d A_a)^2 \tag{2.2.10}$$

where $l_a$ and $r_a$ are the length and radius of the manifold of the pressure retainer. $n_a$ is the number of holes. $\gamma$ is the ratio of the specific heat of the gases in the pressure retainer. $\rho$ is the mass density of the liquid. $C_d$=0.8 is the outlet coefficient of the short tube. $P_0$ and $V_0$ are the initial pressure and volume of the pressure retainer. P is the meta-stable inlet pressure of the pressure retainer during the flight. $\Delta P$ is the pulse pressure difference of the ends of a short tube when resistance $R_a$ is measured. and g is the gravitational acceleration.

(III) Dynamic equations of a pump system (see figure 2.3)

$$\begin{Bmatrix} P_D \\ Q_D \end{Bmatrix} = \begin{bmatrix} m+1+SC_pZ_p & -Z_p \\ -SC_p & 1 \end{bmatrix} \begin{Bmatrix} P_U \\ Q_U \end{Bmatrix} + \begin{bmatrix} -A_UZ_p & -SL_pA_D \\ A_U & A_D \end{bmatrix} \begin{Bmatrix} \dot{X}_p \\ \dot{Y}_p \end{Bmatrix} \tag{2.3.1}$$

where (m+1). $C_p$. $L_p$. $R_p$. $Z_p=R_p+SL_p$ are the dynamic gain of the pump. softness of the gas clock. inertia. resistance and impedance. When (m+1)=1 and $\dot{X}_b=\dot{Y}_b=0$ the above equation has the following form

$$\begin{Bmatrix} P_D \\ Q_D \end{Bmatrix} = \begin{bmatrix} 1+SC_pZ_p & -Z_p \\ -SC_p & 1 \end{bmatrix} \begin{Bmatrix} P_U \\ Q_U \end{Bmatrix} \tag{2.3.2}$$

when Zp=0 (only for the composite parameter $C_p$). the above equation is transformed to

$$\begin{Bmatrix} P_D \\ Q_D \end{Bmatrix} = \begin{bmatrix} 1 & 0 \\ -SC_p & 1 \end{bmatrix} \begin{Bmatrix} P_U \\ Q_U \end{Bmatrix} \tag{2.3.3}$$

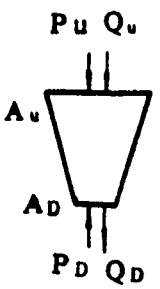


Fig 2.4

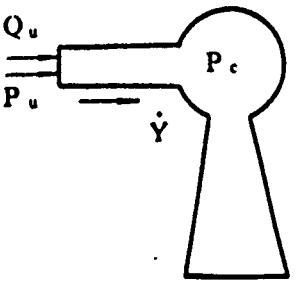


Fig. 2.5

(IV) Related equations for the engine (see figure 2.5)

1. equation for the after-pump pipeline sections (not considering the compressibility of the liquid)

$$\begin{Bmatrix} P_D \\ Q_U \end{Bmatrix} = \begin{bmatrix} 1 & -Z_D \\ 0 & 1 \end{bmatrix} \begin{Bmatrix} P_U \\ Q_U \end{Bmatrix} + \begin{Bmatrix} A_D R_D \dot{Y}_D \\ \end{Bmatrix} \tag{2.4.1}$$

where $Z_D=R_D+SL_D$. and $R_D$. $L_D$ are the resistance and inertia of the after pump pipeline section. and $\dot{Y}_D$ is the pipe wall velocity.

2. equation for the nozzle

When the compressibility of the liquid in the nozzle section is not considered (similar the treatment above). we have

$$P_j=P_C+Z_jQ_j-A_jR_j\dot{Y}_j \tag{2.4.2}$$

where $Z_j=R_j+SL_j$ and $A_j$. $R_j$. $L_j$. and $\dot{Y}_j$ are the cross sectional area. resistance. inertia. and velocity of the nozzle section.

3. combustion chamber

From the combustion thermodynamics. the relation between combustion chamber pulse pressure $P_C$ and two pulse propellant flow rates $Q_j$ and $Q_k$ is

$$P_c=Z_c(Q_j+Q_k) \tag{2.4.3}$$

where $Z_C=H_e/(1+\tau_cS)$, $H_e=C^*/(A_{th}g)$. and $A_{th}$. $C^*$. $\tau_c$, and $Z_C$ are the neck cross sectional area. characteristic velocity. time delay. and impedance.

III. POGO Stability Matrix Algorithm

There are several methods which consider the stability of the system. Most of these methods require the solution of the close-loop/open-loop transfer coefficients and the zeros, polar points and the numbers, and then the stability of the entire close-loop can be analyzed.

The transfer coefficient for some systems can be deduced from the trial method. However, it is very difficult to measure the transfer coefficient of a close-loop system from an unstable close-loop test. Similarly, there are stable and unstable open-loop systems and the determination of their transfer coefficients is equally difficult. Therefore, it is very important to evaluate the system characteristics (close or open loop) based on the composite calculation of the refined model of many sub-systems.

If a pseudo element or pseudo block is introduced into the series of equations of a close-loop system or its block diagram, the characteristic equation of a close-loop or the transfer coefficient and the zero polar point of an open-loop system can be determined in a unified and convenient way. Because the location of the opening is not unique, the introduction of a pseudo block is not unique either. The selection of the location for opening or testing, therefore, should be based on experience. Of course, it is best if the pseudo block can be placed on the main loop of a close-loop system.

Assuming that there is no exterior disturbance, we can obtain a series of equations for the n variables of the n equations of the POGO system as explained in section II. To illustrate this point, assume (or deduce from simplification) that n=3, the following

series of equations (in matrix form) corresponding to block diagram 3.1 is

$$\begin{bmatrix} 0 & D_G(S) & -M_G(S) \\ D_H(S) & -M_H(S) & 0 \\ -K_D & 0 & 1 \end{bmatrix} \begin{Bmatrix} T \\ \dot{X} \\ T' \end{Bmatrix} = [A(S)]\{X\} = 0 \qquad (3.0.1)$$

where

$$[A(S)] = \begin{bmatrix} 0 & D_G(S) & -M_G(S) \\ D_H(S) & -M_H(S) & 0 \\ -K_D & 0 & 1 \end{bmatrix}, \quad \{X\} = \begin{Bmatrix} T \\ \dot{X} \\ T' \end{Bmatrix} \qquad (3.0.2)$$

S is the LaPlace variable, M(S) and D(S) are the corresponding polynomials of the numerator and denominator.

Even though there are many analytical methods for the stability analysis, the basic nature of these methods is similar: namely, the system is stable if the real part of the root of the close-loop characteristic equation if negative, otherwise the system is unstable. Two analytical methods emanate from this point: the close-loop and open-loop analytical method.

1. Direct root-finding from the characteristic equation of the close-loop system

From the real and imaginary parts of the root of the characteristic equation |A(S)|=0, one can determine the stability of a POGO system in any frequency range. Under the perturbation-free condition, the determinant of the variables of the nth order polynomial is zero which is the characteristic system equation. If there is a pseudo block, let $K_D$=1 and one would have

$$|A(S)| = D_G(S)D_H(S) - M_G(S)M_H(S) = 0 \qquad (3.1.1)$$

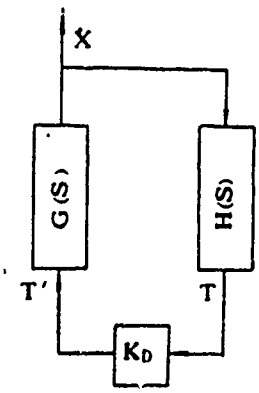


$G(S) = M_G(S) / D_G(S)$

$H(S) = M_H(S)\ D_H(S)$

Fig 3.1

The form of root of the characteristic equation is

$$S_k = S_{kr} \pm jS_{ki} = \omega_k \zeta_k \pm j\omega_k \sqrt{1-\zeta_k^2} \tag{3.1.2}$$

where

$$\omega_k = \sqrt{S_{kr}^2 + S_{ki}^2}\,; \quad \zeta_k = S_{kr}/\omega_k \tag{3.1.3}$$

where $S_{kr}$ and $S_{ki}$ are the real and imaginary parts of the characteristic root: $w_k$ and $\zeta_k$ are the typical frequency and damping ratio of the POGO system in question.

If the damping ratio of the nth modular state of the original real structure is $\zeta_n$, and if the damping ratio of certain modular state is changed from $\zeta_n$ to $\zeta_c$ (while other damping ratios are either kept constant or changed with the same ratio), then we should have at least one neutral stable root (if $S_{kr}=0$) and the width $\Delta$ (dB) of the stable gain of the system is

$$\Delta(dB) = 20 Log_{10}(\zeta_n/\zeta_c), \quad (\zeta_c > 0) \tag{3.1.4}$$

If $\zeta_c < 0$, this would indicate that the system is already a stable device. The system is stable if $\Delta > 0$, whereas the system is unstable if $\Delta \leq 0$.

2. Open-loop analytical method

Taking advantage of the pseudo block method and let $K_D=0$, one can obtain the characteristic equation-polar point equation of the open-loop system

$$A_0(S) = |A(S, K_D=0)| = D_G(S) D_H(S) = 0 \tag{3.2.1}$$

The magnitude and number of the roots of the open-loop characteristic equation can be obtained accordingly. Using the pseudo block but delete the row and column where $K_D$ situated from A(S), then the determinant of one less order can be obtained

$$A_M(S)=|A(S, \text{ delete the row and colume where } K_D \text{ situated}|$$
$$=M_G(S)M_H(S)=0 \qquad (3.2.2)$$

and the number of the zero points and their quantity of the open-loop can be obtained. From $A_D(S)$ and $A_M(S)$, the transfer function $\phi(S)$ of the open-loop can be obtained

$$\phi(S)=\frac{A_M(S)}{A_D(S)}=\frac{M_G(S)M_H(S)}{D_G(S)D_H(S)}=G(S)H(S) \qquad (3.2.3)$$

based on open-loop frequency $\phi(jw)$ and stability analysis. the polar coordinate (Nyquist) diagram. logarithm amplitude diagram. phase-frequency (Bode) diagram. logarithm amplitude-phase (Nichols) diagram can be generated and the stability and width of the POGO system can be determined. (See figures 4.2. 4.3.)

IV. Single-Transfer and Estimation Method of POGO Stability Analysis

POGO has its own special features. In fluid-solid coupled dynamic analysis. some systems require at least two modular vibrational states to cause the unstable vibration of the entire system. For example. the gas dynamic vibration of aircraft wings require bending and twisting vibrational modes. Compared with the inertia and weight of the cross section of the structure. if the gas dynamic force is large enough. then a larger deviation of the

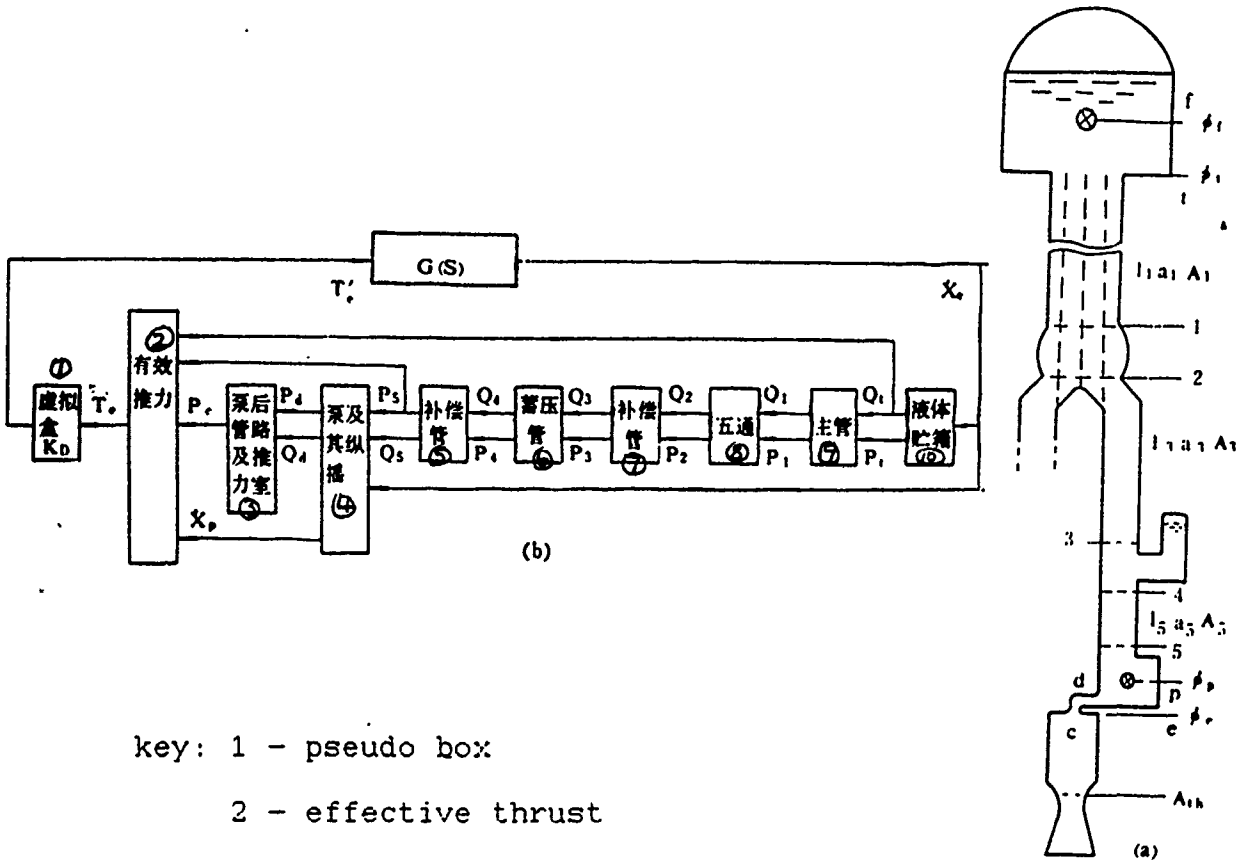


key: 1 - pseudo box

2 - effective thrust

3 - post-pump pipeline and thrust chamber

4 - pump and longitudinal oscillation

5 - compensation pipeline

6 - pressure retaining pipeline

7 - compensation pipeline

8 - five pass

9 - main line

10 - liquid reservoir

Fig 4.1

characteristic frequency of the system can be caused. However, for some other systems such as galloping or pogo. the fluid or pulse dynamic force is relatively small compared with those of larger and heavier structures and only small deviation of the system characteristic frequency can be caused. The stability analysis of these systems can be carried out with single-valence modular state parameter method. In this section. we consider only the single-valence modular state of the rocket structure and the propellent system and use them in the POGO stability analysis. The number of equations involved in greatly reduced in this way. Based on the general feature of the structure of pressure retainer (see figure 4.1), 19 equations for the 19 parameters can be obtained from the discussion in section II. The stability analysis can be carried out using the method discussed in section III; using either the characteristic root of the close-loop equation or the transfer function based on pseudo block principle. One can also carry out parameter elimination from the 19 equations and the transfer equation of the loop in question (see table 4.1) is

$$\dot{X} = G(S)T \tag{4.1}$$

whereas the transfer equation of the feedback loop is

$$T = H(S)\dot{X} \tag{4.2}$$

Then the transfer function of the close-loop with output and feedback is

$$F(S) = G(S)/[1 - G(S)H(S)] \tag{4.3}$$

Table 4.1: Transfer function corresponding to figure 4.1b

key: 1 - tank bottom total outlet cross sectional area / N

$\tau_i = l_i/a_i, \quad L_i = r_i l_i/(A_i g)$

$T_1 = ch(s\tau_1)ch(s\tau_3)+[\tau_1 L_3 sh(s\tau_1)sh(s\tau_3)]/(\tau_3 L_1 N')$

$T_2 = [\tau_3 ch(s\tau_1)sh(s\tau_3)]/L_3+[\tau_1 sh(s\tau_1)ch(s\tau_3)]/(L_1 N')$

$T_3 = ch(s\tau_3)+[\tau_1 L_1 ch(s\tau_1)sh(s\tau_3)]/[\tau_3 L_1 N' sh(s\tau_1)]$

$T_4 = [\tau_3 sh(s\tau_3)]/L_3+[\tau_1 ch(s\tau_3)]/[L_1 N' + h(s\tau_1)]$

$T_{PP} = [ch(s\tau_3)+(Y_e L_3 sh(s\tau_3))/\tau_3]T_1+[T_2 L_3 sh(s\tau_3)]/\tau_3$

$T_{PQ} = [ch(s\tau_3)+(Y_e L_3 sh(s\tau_3))/\tau_3]T_3+[T_4 L_3 sh(s\tau_3)]/\tau_3$

$T_{QP} = [(\tau_3 sh(s\tau_3))/L_3+y_e ch(s\tau_3)]T_1+T_2 ch(s\tau_3)$

$T_{QQ} = [(\tau_3 sh(s\tau_3))/L_3+y_e ch(s\tau_3)]T_3+T_4 ch(s\tau_3)$

$T_P'_Q = [T_{PQ} L_1 sh(s\tau_1)]/\tau_1, \qquad T_Q'_Q = [T_{QQ} L_1 sh(s\tau_1)]/\tau_1$

$N_1(s) = [SP_n(T_{PP}T_Q'_Q - T_P'_Q T_{QP})]/\phi_n(e)$

$D_1(s) = T_P'_Q(SC_P+(m+1)/Z_e)+T_Q'_Q$

$H_1(s) = [(m+1)Z_e/Z_e - A_3\phi_n(p)/(S_e\phi_n(e))]NS_e N_1(s)/D_1(s)$

$H_2(s) = -sNP_n' K_1(s)/D_1(s)$

$K_1(s) = [N_1(s)-(s\mathcal{P}_n D_1(s)T_{PP})\phi_n(e)]/T_P'_Q$

$H_3(s) = 2sNA_1' P_n\phi_n(t)/\phi_n^2(e), \qquad Z_e = Z_r+Z_d+Z_P$

$H_4(s) = -NA_1 C_3 N_1(s),/D_1(s), \qquad E(s) = Z_e(m+1)/Z_r$

$H_5(s) = -C_6 H_2(s)/A'_1$

$C_3 = [m_P\phi_n(tp)\phi_P{}^1 S^2]/[A_3\phi_n(p)F_P(s)$

$C_6 = [m_P\phi_n^2(tp)\phi_P]/2\rho h_1\phi_n(t)\phi_n(f)F_P(s)]$

$P_n = \mathcal{P}_n{}^1 = rh_1\phi_n(f)/g$

$A_1 = A_1' =$ 箱底总出口截面积$/N$ ①

$N' =$ 1 或 4

$\Phi_P = m_P c l_P^2/I_P \qquad \phi_{Pr}' = A_1 d_P^2/I_r$

$F_P(s) = S^2+2\zeta_P\omega_P S+\omega_P^2$

$H(s) = H_1(s)+H_2(s)+H_3(s)+H_4(s)+H_5(s) = H_R(s)+jH_I(s)$

$G(s) = G_n(e)s/(s^2+2\zeta_n\omega_n s+\omega_n^2)$

$\zeta_e = G_n(e)H_R(\omega_n)/(2\omega_n)$

and the open-loop transfer function is

$$\phi(S)=G(S)H(S)=T_{out}/T_{in}=\dot{X}_{out}/\dot{X}_{in} \tag{4.4}$$

where $\dot{X}$, T are the velocity and equivalent thrust of the engine at its normal state. The expressions for G(S) and H(S) are shown in table 4.1.

Based on Norquist stability criteria, the system stability can be determined through the calculation of the characteristic frequency $\phi(jw)$ of the open-loop. From table 4.1 one has

$$G(j\omega)\{[G_n(e)\cos\theta_G]/2\zeta_n\omega_n)\}e^{j\theta_G} \tag{4.5}$$

$$\theta_G=tg^{-1}[(\omega_n^2-\omega^2)/(2\zeta_n\omega_n)] \tag{4.6}$$

$$H(j\omega)=|H(j\omega)|e^{j\theta_H} \tag{4.7}$$

$$\theta_H=tg^{-1}[H_I(\omega)/H_R(\omega)] \tag{4.8}$$

then

$$\phi(j\omega)=\frac{G_n(e)|H(j\omega)|\cos\theta_G}{2\zeta_n\omega_n}e^{j\theta_\phi} \tag{4.9}$$

$$\theta_\phi=\theta_G+\theta_H$$

If this system exhibit $|\phi(jw)|<1$ (or $|\phi(jw)|>1$) for any phase orientation, then this system is stable (or unstable).

If there exists $w=w_C$ and $\theta_\phi(\omega_c)=0$,

$$\theta_G(\omega_c)=-\theta_H(\omega_c) \tag{4.10}$$

and we have

$$|\phi_c|=|\phi(j\omega_c)|=G_n(e)H_R(\omega_c)/(2\zeta_n\omega_n) \tag{4.11}$$

let

$$\zeta_e = G_n(e) H_n(\omega_e)/(2\omega_n) \tag{4.12}$$

based on general control theory, the stable amplitude width $\Delta$(dB) of the system POGO is

$$\Delta(dB) = 20\log_{10}(|\phi(j\omega_e)|)^{-1} = -20\log_{10}(\zeta_e/\zeta_n) = 20\log_{10}(\zeta_n/\zeta_e), (\zeta_e > 0) \tag{4.13}$$

where $\zeta_e$ has the same meaning as before.

If the open-loop frequency is maximum at $\omega = \omega_m$ and

$$|\phi(j\omega)|_{max} = |\phi(j\omega_m)| = |\phi_m| > 1 \tag{4.14}$$

then $\omega = \omega_r$ and

$$|\phi(j\omega_r)| = \frac{G_n(e)|H(j\omega_r)|}{2\zeta_n\omega_n}\cos\theta_G(\omega_r) = 1 \tag{4.15}$$

and we have

$$\theta_G(\omega_r) = \cos^{-1}[2\zeta_n\omega_n/[G_n(e)|H(j\omega_r)|)] \tag{4.16}$$

then the phase width is

$$\theta_r = \theta_H(\omega_r) + \theta_G(\omega_r) \tag{4.17}$$

If system $|\phi_e| < 1$ and $|\Phi_m| > 1$ at non-zero phase orientation, then this is called the phase-orientation stable system and pure phase shift would cause unstable POGO of the system.

So far, except for the assumption of single modular state and single propellent, there is no other assumptions made for the POGO stability analysis. From equations (4.12) and (4.13) we know that

1. the rocket body structure damping ratio $\zeta_n$ is small;

2. the mass is somewhat large or $\omega_{n_1}$ is small;

3. rocket body gain $G_n(e)$ is high; and

4. the real part $H_R(\omega_c)$ of feedback transfer function $H(j\omega)$ is large.

All the factors mentioned above will decrease $\Delta$(dB) and unstable POGO of the system is even more easy to occur. This method and its conclusions also apply to other stability analysis of similar fluid-solid coupling systems.

From the results of the root of characteristic equation and the above analysis, one can realize that the frequency for POGO to occur is very similar to the modular state frequency of rock body structure. In other words, if POGO should occur, the frequency should be around the structure single-valence modular frequency. One can also know that the feedback transfer function of POGO system has its own characteristics: namely, before the measures were taken to overcome the unstable pogo, the characteristic frequency H(jw) is slow-changing with respect to G(jw) and

$$|H(j\omega_c)| \approx |H(j\omega_r)| \approx |H(j\omega_m)| \approx |H(j\omega_n)| \tag{4.18}$$

or

$$H_R(\omega_c) \approx H_R(\omega_r) = H_R(\omega_m) \approx H_R(\omega_n)$$

then we should obtain the following estimation equations

$$\check{\zeta}_c = G_n(e) H_R(\omega_n)/(2\omega_n) \tag{4.19}$$

$$\check{\Delta}(dB) = 20\log_{10}(\zeta_n/\check{\zeta}_c) \tag{4.20}$$

$$\check{\theta}_r = \theta_H(\omega_n) + \cos^{-1}[2\zeta_n\omega_n/(G_n(e)|H(j\omega_n)|)] \tag{4.21}$$

key: 1 - polar coordinate diagram

2 - logarithm amplitude - phase diagram

3 - logarithm amplitude. phase - frequency diagram

4 - $\zeta_c$. $\theta_r$ - frequency diagram

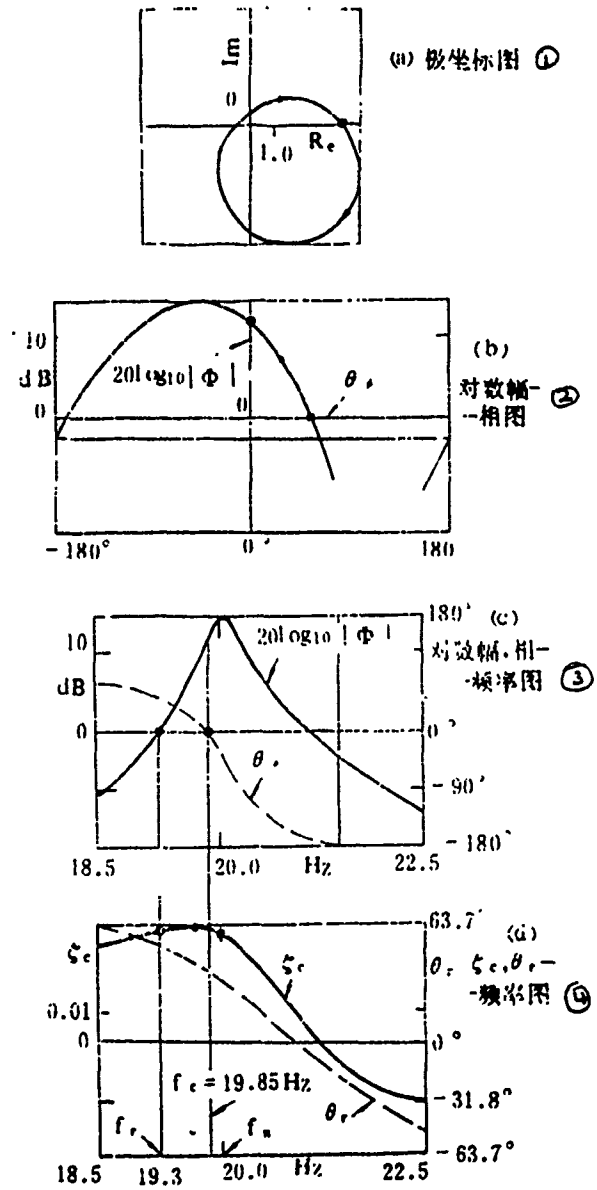


Fig. 4.2: Single-transfer stability analysis of pressure retainer free system ($C_a$=0)

key: 1 - polar coordinate diagram

2 - logarithm amplitude - phase diagram

3 - logarithm amplitude. phase - frequency diagram

4 - $\zeta_c$. $\theta_r$ - frequency diagram

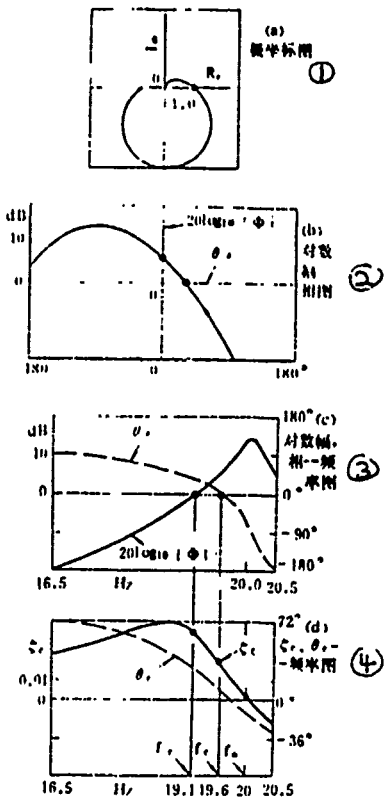

Fig. 4.3: Single-transfer stability analysis of system with pressure retainer ($C_a$=18.57cm$^2$/kg)

Table 4.2: Assumed parameters for space vehicle

(a) 固定参数 ①

| ② 系统 | ④ 密度 $\rho$ $kg\text{-}s^2/cm^4$ | ⑤ 推力室阻力 He (2.4.3)式 $kg\text{-}s/cm^3$ | ⑥ 抽吸管截面积 $A_s$ $cm^2$ | ⑦ 抽吸管长度 $l_s$ cm | ⑧ 声速 $a_s$ cm/s | ⑨ 阻力 $R_p+R_d$ $kg\text{-}s/cm^3$ | ⑩ 惯性 $L_p+L_d$ $kg\text{-}s^2/cm^3$ | ⑪ 振态比 $\phi_o=\phi_p=\phi_f$ | $S_o$(2.1.6)式 $cm^2$ | ⑫ 推力室时迟常数 $\tau_c$ s | ⑬ 振态阻尼比 $\xi_n$ |
|---|---|---|---|---|---|---|---|---|---|---|---|
| ③ 氧化剂 | $1.1584\times10^{-6}$ | $1.459\times10^{-4}$ | 232.25 | 76.2 | $7.112\times10^{4}$ | $4.719\times10^{-4}$ | $3.861\times10^{-6}$ | 1.0 | 1838.6 | .0025 | 0.01 |

(b) 时变参数 ⑭

| ⑮ 系统 | ⑰ 飞行时间百分数 % | ⑱ 振态频率 $\omega_n$ $R_{ad}/s$ | ⑲ 广义质量 $M_n$ $kg\text{-}s^2/cm$ | ⑳ 泵动力学增益 $m+1$ | ㉑ 贮箱液面高度 $h_f$ cm | ㉒ 泵气体柔度 $C_p$ $cm^3/kg$ |
|---|---|---|---|---|---|---|
| 氧化剂 ⑯ | 0 | 72 | 464.31 | 1.0 | 634.99 | 9.322 |
| | 60 | 92 | 89.29 | 1.3 | 279.39 | 46.61 |
| | 80 | 104 | 32.14 | 1.8 | 160.02 | 93.22 |
| | 95 | 126 | 8.929 | 3.0 | 68.58 | 174.79 |
| | 100 | 148 | 4.465 | 5.4 | 38.1 | 349.58 |

key: 1 - fixed parameters

2 - system

3 - oxidizing agent

4 - density

5 - resistance of thrust chamber

6 - cross sectional area of suction pipe

7 - length of suction pipe

8 - speed of sound

9 - resistance

10 - inertia

11 - modular ratio

12 - thrust chamber time-delay constant

13 - modular damping ratio

14 - (b) time dependent parameters

15 - system

16 - oxidizing agent

17 - percentage of time of flight

18 - modular frequency

19 - macroscopic mass

20 - pump dynamic gain

21 - liquid height of liquid reservoir

22 - pump gas softness

Table 4.3

key: 1 - related parameters and pressure retainer parameters in table 4.2 for 95% time of flight

2 - POGO stability equation and calculated results

3 - estimation method

4 - single-transfer method

5 - pressure-retainer free

6 - pressure-retainer

7 - note: Effect of tank-bottom flow is not included.

| 表4.2 95%飞行时间 有关参数及蓄压器参数 ① / 跳振稳定裕度公式及计算结果 ② | | 无蓄压器 ⑤ $R_a=L_a=0$ $C_a=0$ | 有蓄压器 ⑥ $R_a=0$ $L_a=3.432\times10^{-1}kg\text{-}s^2/cm^3$ | |
|---|---|---|---|---|
| | | | $C_a, cm^3/kg$ 90.89 | $C_a, cm^3/kg$ 18.574 |
| 估算法 ③ | 公式(4.19), $\zeta_c$ | 0.03607 | −0.007145 | $1.076\times10^{-3}$ |
| | 公式(4.20), $\Delta(dB)$ | $-11.14dB$ | | $59.36dB$ |
| | 公式(4.21), $\theta_r(Deg)$ | 32.9° | | −11.44° |
| 单传法 ④ | 公式(4.12), $\zeta_c$ | 0.03825 | 0.004296 | 0.01903 |
| | 公式(4.13), $\Delta(dB)$ | −11.65 | 15.62 | −6.0 |
| | 公式(4.17), $\theta_r(D_{eg})$ | 53.71° | | 30.7° |

注 上述参数中不考虑箱底流出量效应。 ⑦

where $\check{A}(dB)$, $\check{\theta}_r$ are the amplitude of the POGO system and the estimated value of the phase-stability width. Following this method, the varying scanning frequency $\omega$ can be manually fixed at the single-valence modular frequency $\omega_{n1}$. If this algorithm is followed, than the amount of calculation is reduced and an overall estimation can be accomplished.

Literatures [4] and [5] have studied the estimation method, however, the error and direction of deviation were not given and there these methods can not be used independently. in table 4.2. a set of aircraft parameters were listed (see [5]) and table 4.3 is the calculational results (with and without pressure retainer) based on parameters in table 4.2. In these calculations, single-transfer and estimation methods were used. Figure 4.2 and 4.3 are the polar coordinate (Nyquist), logarithm amplitude-phase (Nichols), logarithm amplitude, phase-frequency (Bode), and $\zeta_e(f)$ and $\theta_r(f)$-frequency diagrams corresponding to the single-transfer method. From these diagrams, the width of the system stability and the error of single-transfer and estimation methods can be deduced.

From these tables, figures, and calculation experience, it is known that before measures were taken to overcome POGO of space vehicles (such as installation of pressure retainer), estimation method provides good accuracy (relative error smaller than 3dB), however, after overcome measures are taken and estimation method is used to select parameters, the error is large (a few tens of dB) and the results tend to be not as reliable. Therefore, more accurate methods such as single-transfer or the methods explained in section III should be used to check the results.

Another preliminary estimation method for the analysis of POGO stability is to use the characteristic of open-loop frequency $\phi(jw)=G(jw)H(jw)$. When at zero phase orientation, if $w=w_c$ than

$$|H(j\omega_c)| \geq |1/G(j\omega_c)| \tag{4.22}$$

then the POGO system is not stable. If $w_c$ is in the vicinity of the peak frequency $w^*$ of $|H(jw)|$, stability of the system can be determined from the closeness of $w^*$ and $w_n$. Therefore, the first of determining the stability of the system is to obtain the characteristic frequency $w^*$ of $H(jw)$. To make the problem simpler, one can consider the five cross sections t-1-3-5-D of figure 4.1, there are four transfer functions (from section II)

$$\begin{Bmatrix} P_D \\ Q_D \end{Bmatrix} = \begin{pmatrix} 1+SC_pZ_p, & -Z_p \\ -SC_p, & 1 \end{pmatrix} \begin{pmatrix} \mathrm{Ch}\theta_s, & \dfrac{-Z_s \mathrm{sh}\theta_s}{\theta_s} \\ \dfrac{-\theta_s \mathrm{sh}\theta_s}{Z_s}, & \mathrm{ch}\theta_s \end{pmatrix}$$

$$\times \begin{pmatrix} 1, & 0 \\ -Y_e, & 1 \end{pmatrix} \begin{pmatrix} \mathrm{ch}\theta_1, & \dfrac{-Z_1 \mathrm{sh}\theta_1}{\theta_1} \\ \dfrac{-\theta_1 \mathrm{sh}\theta_1}{Z_1}, & \mathrm{ch}\theta_1 \end{pmatrix} \begin{Bmatrix} P_t \\ Q_t \end{Bmatrix} \tag{4.23}$$

based on the "open" ($P_i=0$, $Q_1\neq 0$) or "close" ($P_i\neq 0$, $Q_1=0$) at cross sections t and D, one can obtain the low-frequency and high-frequency resonance equation and formulae for various feedback systems (mainly the pipeline and pump systems).

## V. Analysis and Discussion of Major Parameters

The analysis in this section is based on the related equations in section IV (see table 4.1).

1. outlet flow from the bottom of the tank

Table 4.4

| 部件 ① / 系统参数 / 主要部件 ② | 边界条件 ⑦ | 泵 ㉒ 柔度 ㉓ $C_p$ | 泵 ㉒ 阻力 ㉔ $R_p$ | 泵 ㉒ 惯性 ㉕ $L_p$ | 短管 ㉑ 惯性 ㉗ $L_s$ | 蓄压器 ㉘ 柔度 ㉙ $C_e$ | 蓄压器 ㉘ 惯性 ㉚ $L_e$ | 长管 ⑩ 声速 ㉜ $a_1$ | 参见图 4.1 及§2 节中对应部件传递方程代入边界条件可得如下频率方程或公式 ㉝ |
|---|---|---|---|---|---|---|---|---|---|
| 长抽吸管 ③ | 开闭 ⑧ | | | | | | | $a_1$ | $\cos(\omega l_1/a_1)=0,\ \omega=\pi a_1(1+2n)/2l_1,\ n=0,1,2,\cdots\cdots$ |
| | 开开 ⑨ | | | | | | | $a_1$ | $\sin(\omega l_1/a_1)=0,\ \omega=2n\pi a_1/(2l_1),\ n=1,2,\cdots\cdots$ |
| 长抽吸管，泵 ④ | 开闭 ⑫ | $C_p$ | $R_p$ | $L_p$ | | | | $\infty$ | $\omega_b^2=1/(L_1C_p)$，$\omega_b$为气泡频率 ㉞ |
| | 开开 ⑩ | $C_p$ | | | | | | $a_1$ | $\sin(\omega l_1/a_1)=0,\ \omega=2n\pi a_1/(2l_1),\ n=1,2,\cdots\cdots$ |
| | 开闭 ⑬ | $C_p$ | $R_p$ | $L_p$ | | | | $a_1$ | $\omega^2/\omega_b^2=(\omega l_1/a_1)/t_{an}(\omega l_1/a_1)$ |
| | 开开 ⑪ | $C_p$ | | $L_p$ | | | | $\infty$ | $\omega_p^2=(L_1+L_p)/(L_1L_pC_p)\approx 1/(L_pC_p)$，$(L_1\gg L_p$，高频情况$)$ ㉟ |
| 长抽吸管蓄压器，泵 ⑤ | 开闭 ⑭ | $C_p$ | $R_p$ | $L_p$ | | $C_e$ | | $\infty$ | $\omega_1^2=1/[L_1(C_e+C_p)]$ |
| | 开闭 ⑮ | $C_p$ | $R_p$ | $L_p$ | | $C_e$ | $L_e$ | $\infty$ | $\omega^2=\dfrac{L_1(C_e+C_p)+L_eC_e}{L_1L_eC_eC_p}\approx\dfrac{C_e+C_p}{L_eC_eC_p}$ $(L_1\gg L_e$，高频情况$)$ ㊱ |
| | 开开 ⑯ | $C_p$ | | | | $C_e$ | $L_e$ | $\infty$ | $\omega_e^2=1/(L_eC_e)$ |
| | 闭闭 ⑰ | $C_p$ | $R_p$ | $L_p$ | | $C_e$ | $L_e$ | $\infty$ | $\omega^2=(C_e+C_p)/(L_eC_eC_p)]$ |
| 长抽吸管蓄压器短抽吸管，泵 ⑥ | 开闭 ⑱ | $C_p$ | | $L_p$ | | $C_e$ | | $\infty$ | $\omega_1^2=1/[L_1(C_e+C_p)]$ |
| | 开闭 ㊶ | $C_p$ | | $L_p$ | $L_s$ | $C_e$ | $L_e$ | $\infty$ | $\omega_2^2=(C_e+C_p)/[C_eC_p(L_e+L_s)]$，$(L_1\gg L_s,L_e)$ |
| | 开开 ㊷ | $C_p$ | | | $L_s$ | $C_e$ | $L_e$ | $\infty$ | $\omega_3^2=1/CC_e(L_s+L_e)]$，$(L_1\gg L_s,L_e)$，反共振频率 ㊲ |
| | 闭闭 ㊸ | $C_p$ | | | $L_s$ | $C_e$ | $L_e$ | $\infty$ | $\omega_2^2=(C_e+C_p)/[C_eC_p(L_e+L_s)]$ |

$m+1=1$，$a_3=\infty$，长管惯性为$L_1$，长度为$l_1$ ㊳

key: 1 - component parameters
2 - main component of the system
3 - long suction pipe
4 - long suction pipe. pump
5 - long suction pipe. pressure retainer. pump
6 - long suction pipe. pressure retainer. short suction pipe. pump
7 - boundary condition
8 - open-close
9 - open-open
10 - open-close
11 - open-open
12 - open-close
13 - open-open
14 - open-close
15 - open-close
16 - open-open
17 - close-close
18 - open-close
19 - open-close
20 - open-open
21 - close-close
22 - pump
23 - softness

Table 4.4 (key continued)

24 - resistance

25 - inertia

26 - short tube

27 - inertia

28 - pressure retainer

29 - softness

30 - inertia

31 - long pipe

32 - speed of sound

33 - See figure 4.1 and section II for related transfer function. If suitable boundary conditions are plugged in, the following frequency equations can be obtained.

34 - gas bubble frequency

35 - high frequency condition

36 - high frequency condition

37 - reverse resonance frequency

38 - Long pipe inertia is $L_1$ and length is $l_1$.

When calculate or test the modular states, the tank bottom is either closed or the liquid is not flowing. When the flight POGO analysis is carried out, the tank bottom is opened and the liquid is flowing and, therefore, the contribution of the outlet flow from the bottom of the tank to the macroscopic force should be considered. This is reflected in the $H_2(S)$ and $H_3(S)$ in table 4.1. This factor will contribute to the stability of the system and it is over-conservative if this factor is not considered.

2. local pump longitudinal vibration

The effect of local pump longitudinal vibration is reflected in the contribution to the macroscopic force and is manifested in $H_3(S)$ and $H_4(S)$ terms. When the frequency of the local pump longitudinal vibration $w_p$ is close to or overlapping with the rocket body structural modular state frequency $w_n$, installation of pressure retainer will not suppress POGO. As a result, it is very important to clarify the parameters for local pump longitudinal vibration before flight.

3. composite pre-ump pipeline resonance frequency $w^*$

Experience showed that when the characteristic pre-pump frequency $w^*$ is close to the rocket body structure modular frequency $w_n$, unstable POGO of the system will occur. Hence, to separate $w^*$ far from $w_n$ is one of the important criteria for the design of space vehicles. [9] This can be made clear from the following analysis.

i. When the tank bottom outlet flow and local pump longitudinal vibration are not considered, we have

$$H(S)=H_1(S)=\left[E(S)-\frac{A_s\phi_p}{S_e\phi_e}\right]NS_eA_sI_sE_e(S)N(S)/D(S) \qquad (5.3.1)$$

the meaning of these symbols is explained in table 4.1 and figure 4.1 (same for the following equations).

ii. When there is only one pipeline section and pressure retainer prior to the pump, the D(S) in the above equation takes the form of D(iw) and

$$D(j\omega)=Z_e(j\omega)\left[\frac{\pi\omega/(2\omega_1)}{\mathrm{tg}(\pi\omega/(2\omega_1))}-l_1\omega^2\left(C_p+C_l+\frac{C_a}{1+jC_aR_a\omega}-C_al_a\omega^2\right)\right]+j(m+1)l_1\omega \tag{5.3.2}$$

where $C_t$ is the composite softness of the gas bubbles in the liquid within the pipeline.

iii. When the inertia of the pressure retainer and resistance are not considered, we have

$$D(j\omega)=Z_e(j\omega)\left[\frac{\pi\omega/(2\omega_1)}{\mathrm{tg}(\pi\omega/(2\omega_1))}-\frac{\omega_1}{\omega_b^2}\right]+j(m+1)l_1\omega \tag{5.3.3}$$

where $\omega_1=\pi a_e/(2l_1)$ and is the first valence frequency of the open-close pipeline, and $\omega_b=[l_1(C_e+C_p+C_l)]^{-1/2}$ is the gas bubble frequency.

iv. Let

$$F(\omega)=\frac{\pi\omega/(2\omega_1)}{\mathrm{tg}(\pi\omega/(2\omega_1))}-\frac{\omega^2}{\omega_b^2} \tag{5.3.4}$$

if $w=w^*$, then $F(w^*)=0$ and is called the composite resonance frequency of the pipeline. When $D(jw^*)$ is a minimum, $H(jw^*)$ is a maximum and $\zeta_e(w^*)$ is also a maximum. Therefore, when $w^*=w_n$, unstable POGO of the system would occur very easily. However, it is not true that POGO should always occur because there are other parameters which also control the mechanism (see below).

4. Overlapping of $w^*=w_n$

From above, when 1) the tank bottom outlet flow is not considered. 2) local longitudinal pump vibration occurs. 3) no pressure retainer, and 4) only one section of equivalent pipeline exists prior to the pump, we can have

$$\check{\zeta}_e = G_n(e)H_n(\omega_n)/)\,2\omega_n\tilde{} = \frac{G_n(e)NS_e A_s\phi_p R_e}{2(m+1)\omega_n\phi_e}\left[1+\frac{h_1\phi_f\tau_1\omega_n}{l_1\phi_p\sin(\tau_1\omega_n)}\right]\left[E_g-\frac{A_s\phi_p}{S_e\phi_e}\right]$$

From the above equation, one can learn that even if $w^*=w_n$. $\zeta_e<\zeta_n$ is possible under certain conditions and pogo will not occur. Among these conditions, the gain of the engine $E_g$ is an important parameter. The significance of eq. (5.4.1) is that the effect of related parameters, modular states, or structural gains on the system stability can be determined.

5. parameters and location of pressure retainer

So far there are three methods to select the parameters for pressure retainer

i. reverse resonance frequency method, namely, $w_a=w^*=w_n$;

ii. POGO stability dependability method; and

iii. compromised method, which suppresses the unstable POGO of the system and at the same time keep the typical frequency of pressure retainer line to different from the fixed frequency $w^*\neq w_n$.

From table 4.4, the effect of the parameters and location of pressure retainer on the $w^*$ can be observed. If the pressure retainer is placed near the pump inlet, the efficiency of changing $w^*$ is enhanced and the adjustment of pressure retainer parameters is made easier, while on the other hand, the water impact pressure is reduced and the pressure-reduction due to pre-pump high pulse pressure.

From table 4.4. it is known that after the pressure retainer is added, when the pre-pump pipeline is under the condition of open-close. the first and second valence frequencies $w^*_1$ and $w^*_2$ are

$$\omega_1^* = 1/\sqrt{l_1(C_a+C_p)} \tag{5.5.1}$$

$$\omega_2^* = \sqrt{C_a+C_p}/\sqrt{(l_s+l_a)C_aC_p} \tag{5.5.2}$$

Attention should be paid to the range of applicability of above equations. Generally, $w^*_1$ can be reduced by increasing $C_a$. however. $w^*_2$ can not be increased infinitely by reducing $(l_s+l_a)$ and the $w^*_2$ will be lower than the original second valence frequency (without addition of pressure retainer).

6. equivalent speed-of-sound of pipeline liquid

From (5.3.3), it can be learned that $a_e$ first affect w, then $w^*$, and finally the POGO stability.

Not only is $a_e$ related with the property of the liquid. it is also related with the gas content $V_g$ generated during the flow process. pipeline material. and boundary supporting conditions. When the volume of liquid in the pipeline is $V_l$. the total volume is $V=V_lV_g$ and the composite density $\rho$ is

$$\rho = \rho_l V_l/V + \rho_g V_g/V \tag{5.6.1}$$

and the composite elastic modulus K and $a_e$ are

$$K = K_l/[1+(V_g/V)(K_l/K_g-1)] \tag{5.6.2}$$

$$a_e = \sqrt{K/\rho}/\sqrt{1+(K/E)(D/\delta)C} \tag{5.6.3}$$

where D. $\delta$, E. $\mu$ are the inner diameter. thickness. elastic modulus. and Poisson's ratio of the pipeline material. Note that C

is related with the boundary supporting condition. When the upstream end of the pipeline is fixed and the downstream end is free. C=1-$\mu$/2; when there is no axial strain of the entire pipeline, C=1-$\mu^2$; when there is not axial stress, C=1.

The gas content in the pipeline liquid $V_g/V$ and the theoretical and experimentally obtained $a_e$ curves are shown in figure 5.1. [10]

7. pre-pump liquid gas content softness $C_l$ and pump gas softness $C_p$

From (5.3.3), the major factors influencing $w_b$ is $C_l$ and $C_p$. Theoretical determination of these quantities is difficult and only experimental method can be applied. Based on the experimentally determined $w^*$ and $w_l$ and through equation (5.3.4) ($F(w^*)=0$), $w_b$ can be obtained and $C_l+C_p$ can be calculated.

8. boundary condition of pre-pump pipeline

Generally, when the characteristic frequency of the pre-pump pipeline is calculated or experimentally determined, the effect of the boundary supporting conditions (both ends) is significant. However, in POGO calculation, the boundary condition of the connection between pipelines is not clearly defined. This is because the boundary condition should be determined by the continuous condition of the system loop. For example, when $C_a+C_p+C_l=0$, from eq. (5.3.4) $F(w^*)=0$

$$\omega^*=\pi a_e(2n-1)/(2l_1),\ n=1,\ 2\cdots \tag{5.8.1}$$

and this corresponds to the open-close boundary condition. Similarly, when $Ca+Cp+C_l\approx\infty$, then

key: 1 - test

2 - theory

3 - static pressure

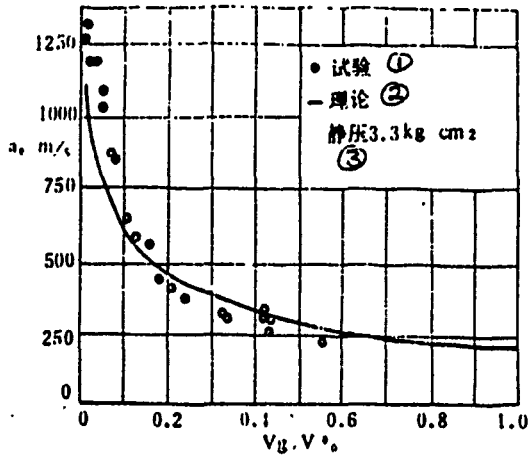


Fig. 5.1: Relationship between speed of sound $a_e$ and gas bubble content $V_g/V$

$$\omega^*=n\pi a_o/l_1,\ n=1,\ 2,\ \cdots \tag{5.8.2}$$

and this corresponds to the open-open boundary condition. In reality.

$$0<C_a+C_p+C_l<\infty \tag{5.8.3}$$

and if $F(w^*)=0$ is used to calculate composite resonance frequency of the pipeline, then we should come up with the boundary condition for either open-open nor open-close.

9. dynamic gain (m+1) of the pump

Dynamic gain of the pump is one of the quantities that is somewhat difficult to determine. It affects the gain of the engine $E_g$ and other quantities (see eq. 5.4.1) and furthermore, the system stability. One of the key parameters in POGO calculation is m+1. From the relationship of the variables in section II, we have

$$(m+1)=Z_a(j\omega)P_D/[P_u(Z_a(j\omega)+Z_D(j\omega)] \tag{5.9.1}$$

where $Z_C$, $Z_D$, $Z_e$ (see table 4.1) can be obtained from calculation. $P_u$ and $P_D$ are the pressure pulse before and after the pump, which can be obtained from experiment.

10. gain of the engine $E_g$

From eq. (5.4.1), when $E_g<A_5o_p/(S_eo_e)$, we have $\zeta_a<0$ and the design of the engine is adequate. No POGO will occur even if the resonance frequency $w^*$ of the pre-pump pipeline is overlapped with $w_n$. This is also one of the most important design criteria for the engine of space vehicles.[11]

11. gain of rocket body structure $G_n(e)$

The structure gain $G_n(e)$ can be defined based on eq. (2.1.3) and from eq.s (4.12) and (5.4.1), it can be seen that $\zeta_e$ or its estimated value $\check{\zeta}_e$ are proportional to $G_n(e)$. Since $G_n(e)$ can be expressed in terms of the time-of-flight as $G_n(e,t)$, therefore, the trend of $\zeta_e(t)$ and $\check{\zeta}_e(t)$ is similar to that of $G_n(e,t)$ and the accuracy of the result can be determined. Gain of rocket body structure is also one of the key parameters in POGO design. Sometimes even slight change in the structure modular frequency will result in significant change in structure gain.

12. structure modular damping ratio $\zeta_n$

$\zeta_n$ consists of three parts: fluid damping, material damping, and structure damping. It can be learned from eq.s (3.1.4), (4.13) and (4.20) that the magnitude of $\zeta_n$ has a direct effect on the accuracy of POGO stability analysis. Hence, this parameter is an important parameter and is generally provided by test or experience. The test result, even if identical method were used, will show discrepancy. The discrepancy of the $\zeta_n$ of same order based on various methods will be even greater. In reference [12], $\zeta_n$ was obtained based on various test and processing techniques and the discrepancy is very significant. From a broader prospective, decreases with modular frequency as shown in figure 5.2. [12] If high vacuum, low gravity, and other conditions that can not easily simulated on earth is considered, it is even more obvious that dependability analysis of $\zeta_n$ should be carried out. Because of the difference in test methods, boundary supporting conditions, payload conditions, and the non-linear effects, the $\zeta_n$ obtained from the full scale test will show large discrepancy and is not dependable.

key: 1 - sinusoidal fixed frequency test data

2 - 4 excitors random test data

3 - 3 excitors random test data

4 - 90% of the data are lower than this line

5 - modular damping ratio

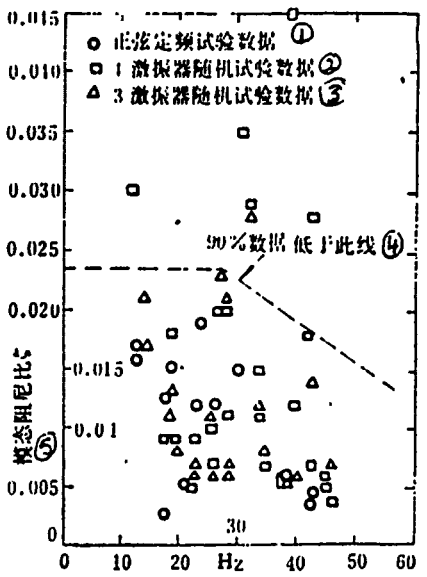


Fig. 5.2: Modular damping ratio obtained from various methods

Even though in the stability calculation, the value of $\zeta_n$ is taken to be 0.01 and 0.007 by groups in USA and France, respectively, it is generally believed that it is not over-conservative even if a lower value of $\zeta_n$ is used. If the suppression of POGO is difficult using other methods, the increase in damping ratio of the key parts of the rocket structure, the modular damping $\zeta_n$ of the overall rocket structure will be increased and POGO can be suppressed. [13]

13. comparison of the importance of various structural modular parameters of different orders

The importance of the structural modular parameters of certain order is evidently determined by the actual problems encountered. For example, if the structural response to the acute bottom seat vibration (for aircraft or satellites) is considered, the modular-state related parameters such as "effective mass" is an important basis for the determination of the importance of certain modular states. For the POGO problem, the modular states which cause POGO are obviously the important states. They are:

i. large mass, low frequency $w_n$;

ii. higher structural gain $G_n(e)$;

iii. small modular damping ratio $\zeta_n$; and

iv. modular states which make $w^*$ close to $w_p$.

## VI. Dependability of POGO Stability Calculation

The design of space vehicles is based on the nominal values of various parameters. In reality, all the parameters will deviate from the nominal value. The test value of a certain parameter will also depend on the location, time, installation method, temperature,

humidity, and status of the instrument. Furthermore, the result will be different if test methods is different.

Since the development cost of space vehicle is huge, to guarantee flawless design, the dependability calculation and analysis is important. If a new product is involved, the test data may be scarce, the correct data may be difficult to obtain from theoretical calculation or from a single test. Often it would require a lot of man-power, a long preparation period, and a tremendous budget for a particular test which may be extremely contaminating to the environment. For the systems which include parameters of this kind, it is better to use the computer to carry out a Monte Carlo system dependability analysis.

From sections II and III, it is clear that there are many primitive parameters involved in the dependability analysis and each parameter has its own probability distribution. The combination of all the parameters represents a simulated flight and the dependability analysis for this particular flight can be carried out. Hence, the combination of random sampling of all the parameters (based on its probability distribution) and the estimation criterion for unstable POGO will generate n sets of parameters which represent n times of simulated flight. The POGO stability analysis for these n flights can be proceeded and than the probability of unstable POGO can be calculated based on some credibility criterion.

There are constants, time-dependent constants, random constants of various probability distribution, and time-dependent random constants in a POGO system. For example, modular state damping ratio $\zeta_n$ exhibits the minimum-value distribution, pump dynamic gain (m+1)

exhibits the maximum-value distribution. pump gas softness $C_p$ and pipeline equivalent speed-of-sound $a_e$ exhibit normal distribution. The sampling method for these parameters are:

$$\zeta_{nj}=U_n+B_n\ln\ln[1/(1-R_{nj})],\ j=1,\ 2,\ \cdots n \tag{6.1}$$

$$(m_j+1)=U_k-B_k\ln\ln[1/R_{kj}],\ j=1,\ 2,\ \cdots n \tag{6.2}$$

$$a_{ej}=\mu_e+\sigma_e S_{cj}\quad j=1,\ 2,\ \cdots n \tag{6.3}$$

where $U_n$. $U_K$. $B_n$. $B_K$ can be determined by the estimated values of related overall parameter and $R_{nj}$ and $R_{kj}$ are the number of uniform-divisions. $\mu_e$ and $\sigma_e$ are the averages of related overall parameters and estimated value of standard deviation. $S_{cj}$ is the normal state random number and j is the designation of the random state.

From section V. one learns that some of the parameters are important but difficult to determine. If sampling is carried out for all the parameters. and then POGO stability analysis conducted for all the combinations (while the flight condition is changed in unit of second). the amount of calculation will be significant. From experience. some of the undetermined parameters can be manually reduced or combined to reduce the amount of calculation. Likewise. the number of combinations can be reduced or the flight simulation can be carried out based on a longer time unit.

## VII. Criteria for POGO Stability and Dependability

It can be seen from sections III and IV that POGO stability is determined by the amplitude width $\Delta$(dB) and phase width $\theta_r$(degree).

The criterion for POGO stability is similar to the control system: namely, amplitude width $\Delta$>6dB and phase width $|\theta_r| > 30^\circ$.

This corresponds to the structural safety consideration of design safety coefficient of 2. However, this stability width can not be extended to uncertain parameters such as $\zeta_n$, $C_p$, or (m+1) and dependability statics should be employed. Under these circumstances, the criterion for POGO stability is $3\sigma$; namely, the probability of unstable POGO as a result of the random combination of all the parameters is less than 0.00135.

From above, it can be concluded that a better dependability criterion of POGO stability is for the nominal widths to be $\Delta \geq 6$dB and $|\theta_r| > 30^\circ$ in addition to the acceptable probability of unstable POGO of $P<0.00135$.

## VIII. Conclusions

1. When the space vehicle engine pulse thrust frequency and the rocket body structural frequency ($w^*$ and $w_p$ or $w_n$) are near or overlapped and the structural gain is sufficient, then the pulse motion of the liquid in the fuel tank is equivalent to the pulse excitor and it becomes as a source of excitation for the thrust system behind the tank bottom. This constitutes a positive feedback system. The simplest model for this system is the free-free double mass-spring-damper system. This model connects the POGO stability damper analysis principles based on various methods.

2. After the dynamic equations of POGO system are introduced, the POGO matrix analytical method, computer calculation of open-loop transfer function, POGO single-transfer method and estimation method are explained. These methods can be used in various design stages and can be complementary to one another. Through the use of

examples, accuracy of the estimation method is evaluated before suppressing measures were taken. However, after suppression measure parameters are selected (or during selection), the application of estimation method should be cautioned and calibration with more accurate methods should be performed.

3. Analysis and discussion of some important parameters is given in section V. This section also points out some of the important parameters in the design of space vehicles, engine system, or the suppression measures of unstable POGO. Furthermore, the various measures for suppressing POGO is discussed.

4. Dependability analysis should be carried out for POGO stability analysis. Based on the test data and test experience, the computer simulation (such as Monte Carlo method) can be used for the dependability analysis. The criterion for the POGO stability/dependability is such that the nominal width $\Delta \geq 6dB$ and $|\theta_r| \geq 30^\circ$ plus the probability of unstable POGO $P < 0.00135$.

REFERENCES

[1] Anon: Prevention of Coupled Structure-Propulsion Instability (POGO), NASA Space Vehicle Design Criteria (Structures), Sp-8055, 1970

[2] Rasumoff, A. and Wanje, R. A.: The POGO Phenomenon: Its Causes and Cure, Astronautical Research, 1971

[3] NASA ad Hoc Study Group: Structural Dynamics Technology Research in NASA: Perspective and Future Needs. N79-21450. 1979

[4] Rubin, S.: Longitudinal Instability of Liquid Rockets due to Propulsion Feedback (POGO). J. Space-craft Rockets. Vol. 3 No. 8 Aug. 1966

[5] Lewis W.: Simplified Analytical Model for Use in Design of Pump-Inlet Accumulators for the Prevention of Liquid-Rocket Longitudinal Oscillation (POGO). NASA TN D-5394. 1969

[6] Rubin. S., Wanger. R. G., and Payne. J. G.: POGO Suppression of Space Shuttle-Early Studies. NASA CR-2210 1973

[7] S. Kobayashi and K. Kojima: Longitudinal Self-Exited Vibration of Liquid Prepellant Launch Vehicles (POGO). IAF-81-393. 1981

[8] Fung. Y. C.: An Introduction to the Theory of Aeroelasticity. J. Wiley & Sons. Inc., New York. 1955

[9] Norquist. L. W. S., Marcus J. P. and Ruscio. D. A.: Development of Close-Coupled Accumulators for Suppressing Missile Longitudinal Oscillations (POGO). AIAA Paper No. 69-547. 1969

[10] Wylie. E. B. and Streeter. V. L.: Fluid Transient. McGaw-Hill Book Co., New York. 1978

[11] Fenwick. J. R., Jones J. H. and Jewell. R. E.: Space Shuttle Main Engine (SSME) POGO Testing and REsults. S & V Bulletin 52-2. 1982

[12] Chen. J. C.: Evaluation of Model Testing Methods. AIAA 84-1071-Cp. May 1984

[13] Poizat. M., Vialatoux. P., Cochery. P. and Vedrenne. M.: Viscoelastic Damping System Use as a remedy for POGO Effect on

the Diamont Satellite Launch Vehicle. Shock and Vibration Bulletin 46. Part 2. August 1976. pp.245-266

## DISTRIBUTION LIST

## DISTRIBUTION DIRECT TO RECIPIENT

| ORGANIZATION | MICROFICHE |
|---|---|
| B085 DIA/RTS-2FI | 1 |
| C509 BALL0C509 BALLISTIC RES LAB | 1 |
| C510 R&T LABS/AVEADCOM | 1 |
| C513 ARRADCOM | 1 |
| C535 AVRADCOM/TSARCOM | 1 |
| C539 TRASANA | 1 |
| Q592 FSTC | 4 |
| Q619 MSIC REDSTONE | 1 |
| Q008 NTIC | 1 |
| Q043 AFMIC-IS | 1 |
| E051 HQ USAF/INET | 1 |
| E404 AEDC/DOF | 1 |
| E408 AFWL | 1 |
| E410 ASDTC/IN | 1 |
| E411 ASD/FTD/TTIA | 1 |
| E429 SD/IND | 1 |
| P005 DOE/ISA/DDI | 1 |
| P050 CIA/OCR/ADD/SD | 2 |
| 1051 AFIT/LDE | 1 |
| CCV | 1 |
| P090 NSA/CDB | 1 |
| 2206 FSL | 1 |

Microfiche Nbr: FTD91C000705
FTD-ID(RS)T-0572-91